REFERENCES

1. L. Spitzer and R. Härm, *Phys. Rev.* **89**, 977 (1953).

2. S. I. Braginskii, in *Reviews of Plasma Physics*, edited by M. A. Leontovich, (Consultants Bureau, New York, 1965) Vol. 1, p. 205.

3. R. C. Malone, R. L. McCrory, and R. L. Morse, *Phys. Rev. Lett.* **34**, 721 (1975).

4. D. R. Gray and J. D. Kilkenny, *Plasma Phys.* **22**, 81 (1980).

5. A. R. Bell, R. G. Evans, and D. J. Nicholas, *Phys. Rev. Lett.* **46**, 243 (1981).

6. W. M. Manheimer, *Phys. Fluids* **20**, 265 (1977).

7. D. R. Gray et al., *Phys. Rev. Lett.* **39**, 1270 (1977).

8. J. A. Stamper et al., *Phys. Rev. Lett.* **26**, 1012 (1971).

9. D. W. Forslund and J. U. Brackbill, *Phys. Rev. Lett.* **48**, 1614 (1982).

10. M. A. Yates et al., *Phys. Rev. Lett.* **49**, 1702 (1982).

11. D. Shvarts, J. Delettrez, R. L. McCrory, and C. P. Verdon, *Phys. Rev. Lett.* **47**, 247 (1981).

12. I. P. Shkarofsky, T. W. Johnston, and M. P. Bachynski, *The Particle Kinetics of Plasmas* (Addison-Wesley, Reading, Massachusetts, 1966).

13. I. P. Shkarofsky, *Phys. Rev. Lett.* **42**, 1342 (1979).

14. M. Strauss, G. Hazak, D. Shvarts, and R. S. Craxton, in Proceedings of the CECAM Workshop on "The Flux Limiter and Heat Flow Instabilities," Paris, 1982 (unpublished).

15. J. A. Stamper and B. H. Ripin, *Phys. Rev. Lett.* **34**, 138 (1975); J. A. Stamper, E. A. McLean, and B. H. Ripin, *ibid.* **40**, 1177 (1978); A. Raven, O. Willi, and P. T. Rumsby, *ibid.* **41**, 554 (1978).

2.C   Statistical Ray Tracing in Plasmas with Random Density Fluctuations

Statistical ray tracing is a method of describing the random behavior of light rays in a plasma in terms of the statistical properties of the random electron density component. As in the earliest random-medium propagation formalisms, this method is based on the use of geometrical optics to sample the random density fluctuations with light rays.[1-3]

The random-walk spreading of beams of light due to random density fluctuations is of interest to laser fusion because spreading reduces small-scale illumination nonuniformities and because the efficiencies of various energy absorption mechanisms lose some of their angle-of-incidence dependence as the beam acquires a wider angular distribution. Such considerations could affect target illumination uniformity, which is a crucial quality factor in the success of high-compression implosions.[4] The results of virtually any laser-plasma interaction experiment where properties of reflected or transmitted light are being measured are bound to be affected at some level by random density fluctuations. The use of the spreading of transmitted or reflected laser beams as a corona-structure diagnostic is not without precedent; Chandrasekhar[1] was among the first to use the random motion and scintillation of stellar images to obtain estimates of the relevant scale lengths and density fluctuation amplitudes of the turbulent atmospheric layer causing this behavior.

The theory of wave propagation in random media has advanced beyond the geometrical-optics formalisms[2,3] and has been applied to ionospheric scattering[5] and marine acoustics.[6] Even though our immediate concern is laser fusion, it should be noted that the work to be described in this article is potentially applicable to wave propagation in random media in other physical contexts.

An important result of our work has been the extension of statistical ray-tracing techniques to problems where the non-random "background" density component is inhomogeneous. It has been found that a strongly refracted beam of light will not only spread due to the random density fluctuations; its mean (center) ray will also drift slightly from the path taken by the unperturbed, zero-fluctuation ray path. To our knowledge, such a drift has never been derived or described in a statistical ray-tracing theory, but it is a necessary part of a quantitatively complete beam-propagation theory. A drift term has been formally expressed in a wave diffusion theory by Carnevale et al., but this term was not evaluated for circumstances general enough to give a nonzero result for this effect.[7]

The calculation of energy absorption efficiencies in the presence of density fluctuations superimposed upon an idealized density profile has been considered elsewhere for coherent disturbances of the density profile[8] and for random density fluctuations confined to restricted regions along density gradients near the critical surface where resonance absorption occurs.[9,10] The formalism to be discussed here deals more directly with the propagation of the light and considers random density fluctuations throughout the plasma, so that the results depend upon the statistical properties of the plasma as a whole, rather than on a restricted class of coherent density ripples or on fluctuations in a restricted region.

To demonstrate the use and validity of statistical ray-tracing, results for the evolution of intensity profiles of beams incident on a plane-parallel linear-profile plasma will be presented and compared with numerical Monte-Carlo results.

The statistical-ray-tracing approach is applicable only to problems where the electron-density profile can be decomposed into a non-fluctuating component and a random component that gives each ray in a beam of light a random perturbation. In hydrodynamic simulation codes, the light intensity distribution is often computed by tracing an ensemble of rays, ray by ray, through the plasma. The electron-density information from such codes does not include an identification of random and non-fluctuating components, but the statistical-ray-tracing method could be useful if such a decomposition could be postulated *ad hoc.* For example, one could model the effects of fluctuations whose scale lengths are too short to be resolved by a computational fluid mesh. In the illustrative example to be considered below, the non-fluctuating, unperturbed density component is represented by an idealized analytic form. This allows the intensity profile of a beam of light to be expressed in terms of the solution of a set of coupled ordinary differential equations. This simplification makes it relatively easy to study the dependence of the evolution of a beam on the statistical parameters of the density fluctuations; a much greater effort would be required to obtain a large data base from Monte-Carlo calculations.

Statistical Ray-Tracing Theory

To calculate the behavior of a statistical ensemble of perturbed ray trajectories, one begins with the geometrical optics ray equation[11]

$$\mu \frac{d}{ds} \mathbf{v} = \nabla\mu - \mathbf{v}\,(\mathbf{v} \cdot \nabla\mu), \tag{1a}$$

$$\mu = (1 - n_e/n_c)^{1/2} \tag{1b}$$

for the deflection of the ray direction vector $\mathbf{v}$ at a point along the ray trajectory specified by the path-length parameter s. The index of refraction μ is given here in terms of the electron density n_e and the critical electron density n_c. The ray equation relates ray-trajectory perturbations to zero-mean density perturbations δn superimposed upon a background density n_0, where

$$n_e = n_0 + \delta n, \tag{2a}$$

and

$$<\delta n> = 0. \tag{2b}$$

The brackets here denote a local average. This perturbation approach requires that the rms amplitude of the density fluctuations, σ, be small so that the relative fluctuations of the index of refraction are small. This condition is simply

$$\sigma \ll n_c - n_0, \quad \text{or} \quad \delta\mu/\mu \ll 1, \tag{3a}$$

where

$$\sigma^2 = <\delta n^2>. \tag{3b}$$

The density fluctuations are characterized by a correlation length h that must be much smaller than the overall scale length L of the problem. For the present, a suitable example is

$$<\delta n \, (\mathbf{x}) \, \delta n \, (\mathbf{x} + \Delta \mathbf{x})>$$

$$= \sigma(\mathbf{x}) \, \sigma(\mathbf{x} + \Delta \mathbf{x}) \, \exp \left(- \Delta \mathbf{x} \cdot \Delta \mathbf{x} / h^2 \right), \tag{4a}$$

where

$$h \ll L \sim n_0 / | \nabla n_0 | \sim \sigma^2 / | \nabla \sigma^2 |. \tag{4b}$$

This example contains a long-scale-length spatial dependence in addition to the short-scale-length Gaussian cutoff.

By passing a sequence of rays from a pencil beam through a large sample of these fluctuations, the following equation for the mean-ray direction vector $<v>$ is obtained:

$$\frac{d}{ds} <\mathbf{v}> = - \frac{[\nabla n_0 - \mathbf{v} \, (\mathbf{v} \cdot \nabla n_0)]}{2 \, (n_c - n_0)}$$

$$+ \frac{[\nabla \sigma^2 - \mathbf{v} \, (\mathbf{v} \cdot \nabla \sigma^2)]}{8 (n_c - n_0)^2} - \frac{\pi}{2} \frac{\sigma^2}{h(n_c - n_0)^2} \mathbf{v}. \tag{5}$$

Each ray has the same initial direction vector v. Equation (5) is obtained by integrating Eq. (1a) over a path interval that is small in comparison with the overall scale length of the problem, yet long enough in comparison with the correlation length, so that the non-accumulating effects of the fluctuations average out. In obtaining Eq. (5), Eqs. (1) and (2) must be iterated at least once for the lowest-order nonzero fluctuation effects to appear.

The first term in Eq. (5) represents the refraction of the rays due to the unperturbed density gradient. The second term represents an additional drift due to the gradient of the fluctuation amplitude, and the third term represents the foreshortening of the mean direction vector due to the spreading of the individual rays away from the mean direction. The net shift and spreading occur because correlations in the density fluctuations cause the random impulses to fortuitously reinforce each other. It is significant that no drift effect due to the simultaneous presence of density fluctuations and a nonzero background gradient is found. The slowing term due to the spreading of the beam agrees with the earliest results in ray statistics.[1,2]

The angular spreading rate of the light beam is obtained by solving Eq. (1a) to lowest order in δn and forming the ensemble average of the square of the ray deflections. This gives

$$\frac{d}{ds} <\mathbf{v}_\perp \cdot \mathbf{v}_\perp> = \pi^{1/2} \frac{\sigma^2}{h(n_c - n_0)^2} \,, \tag{6}$$

which is the growth rate of the mean-square angular radius of the ray distribution. The growth rate is just what one would expect for a random walk in the profile plane where each ray receives a random angular displacement of roughly $\sigma/(n_c-n_o)$ radians from each independent fluctuation it traverses, or, equivalently, once per correlation length h along its path. The total rms angular displacement is essentially the displacement due to one impulse, or one fluctuation, multiplied by the square root of the number of impulses, just as is indicated by the form of Eq. (6).

Solving an Illustrative Problem

The problem to be considered below is that of a beam spreading as it refracts through a plane-parallel uniform-gradient plasma. The solution is cast in the form of an elliptical Gaussian ray distribution in the profile plane of the beam. This plane is represented in Fig. 17 by the X-Y axes placed normal to the trajectory of the mean ray, $\mathbf{x}$ (s), at the point denoted by s. The unperturbed trajectory $\mathbf{x}_o(s)$ is assumed to be known from the solution to this problem for $\sigma=0$. The displacement of the mean ray from the unperturbed trajectory can be found by integrating the beam shift term in Eq. (5). The beam profile distribution is centered on the mean ray and is represented in Fig. 17 by an iso-intensity surface, such as the rms beam-radius surface. The evolution equation for this distribution is calculated by propagating each infinitesimal phase-space element of the distribution an infinitesimal distance while allowing each element to broaden at the rate given by Eq. (6). The evolution equation itself and the details of its derivation and solution will be presented elsewhere. The beam-profile intensity distribution can be written in terms of the profile-plane phase space $(\mathbf{X}_\perp, \mathbf{V}_\perp)$ in the form

$$f(\mathbf{X}_\perp, \mathbf{V}_\perp) \propto \exp\left\{-\left[\frac{X^2}{a_x(s)} + \frac{2XV_x}{b_x(s)} + \frac{V_x^2}{c_x(s)}\right]\right.$$

$$\left. -\left[\frac{Y^2}{a_y(s)} + \frac{2YV_y}{b_y(s)} + \frac{V_y^2}{c_y(s)}\right]\right\}, \tag{7}$$

where either of the principal (X or Y) axes remains in a plane parallel to the constant-density surfaces of the unperturbed plasma as the refraction of the mean beam rotates the profile plane. The evolution equation for f reduces to a set of coupled ordinary differential equations for the six parameters in Eq. (7), $a_x(s)$, $a_y(s)$, etc. For cases without the high degree of symmetry of the plane-parallel problem, more parameters may be needed.

Statistical and Monte-Carlo Results for the Illustrative Problem

The plane-parallel plasma considered here is illustrated in Fig. 18 with superimposed isodensity contours for typical density fluctuations with constant rms amplitudes of 4% and 1% of the critical density. Density fluctuations such as these are generated for the Monte-Carlo

solutions to this problem. These fluctuations are expressed within the Monte-Carlo calculation as a Fourier series with component amplitudes set according to the discrete spectrum needed to give the correlation function in Eq. (4a) and with phases taken from a random-number generator. The Fourier components in frequency space are chosen such that the fluctuations and the correlation function are periodic in space with the period chosen to be equal to one scale length L. The electron density can be written as

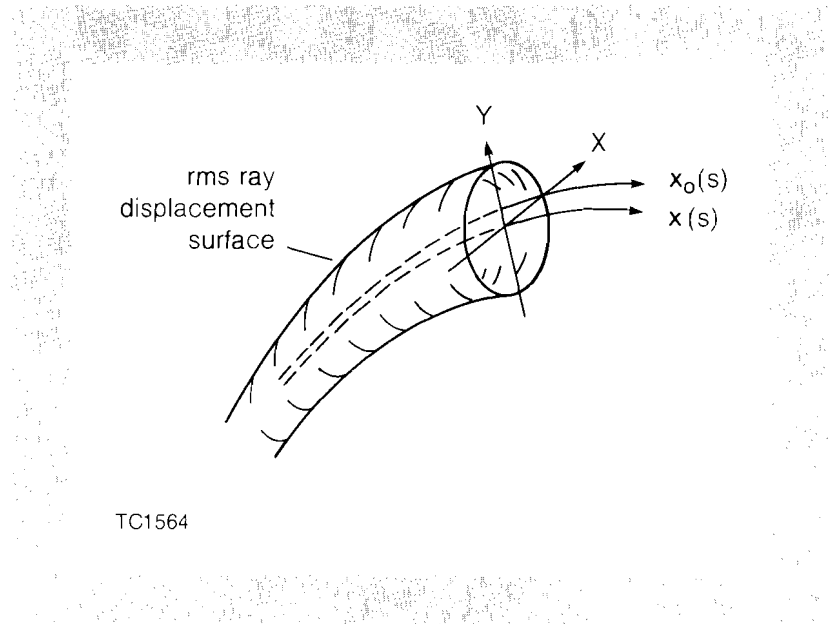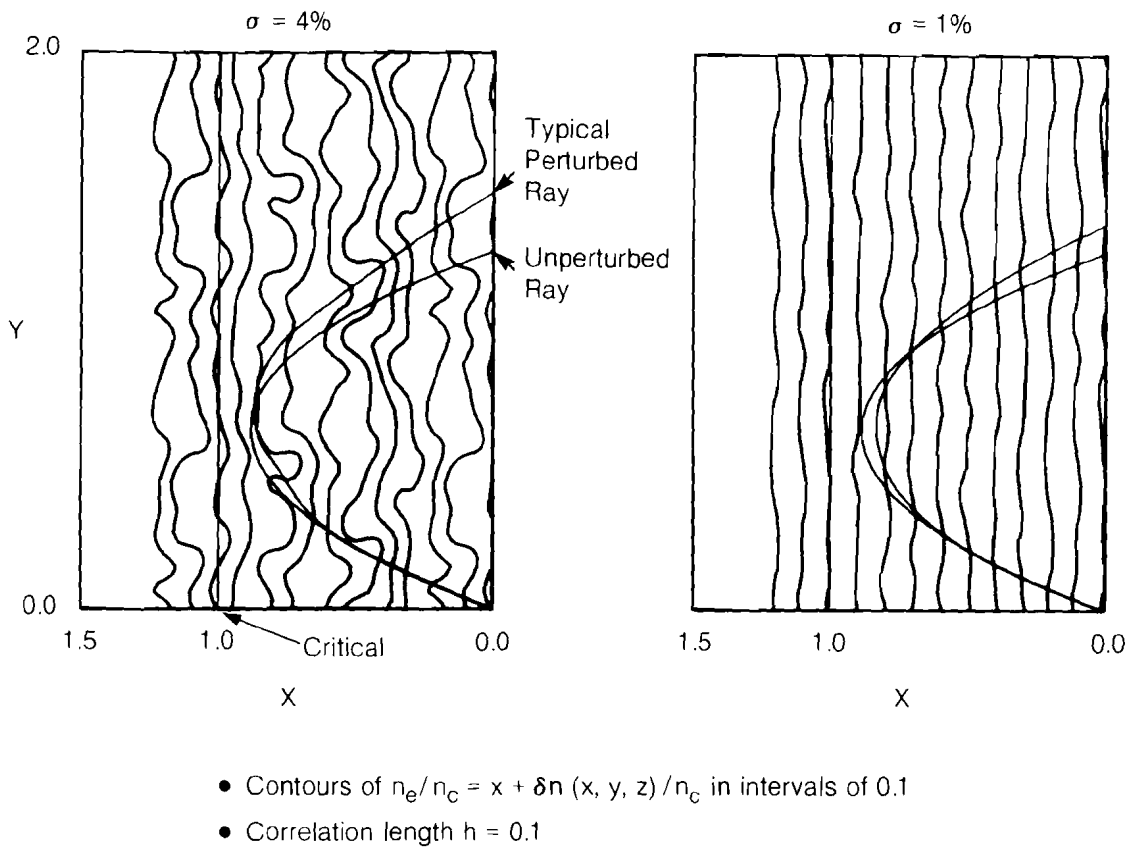$$n_e = (x/L)n_c + \delta n(x, y, z). \tag{8}$$

TC1564

Fig. 17
A statistical description of a light beam consists of an intensity distribution in the phase space transverse to the mean ray trajectory, x(s), at a point specified by the path-length parameter s. The mean ray is generally shifted from the path of the unperturbed ray, $x_0(s)$. The beam envelope, defined by the rms displacement of rays from the mean ray along any direction in the profile plane, provides a concrete visualization of the beam.

The correlation length in this example is chosen to be $h/L = 0.1$. Each frame in Fig. 18 shows how a typical ray wanders from the unperturbed path due to these fluctuations.

Figure 19 shows how 49 different rays propagate through these same two plasmas. For each ray, the phases of the fluctuation Fourier components are changed. The rms spatial widths of these beams calculated according to the statistical-ray-tracing method can be used to construct the rms beam envelope. The boundaries of this envelope in the plane of refraction of the unperturbed ray are drawn in Fig. 20 so that Figs. 19 and 20 can be compared by superposition. Most of the Monte-Carlo rays lie within the rms boundaries. It is interesting to note that qualitative features, such as the focusing of the beam just after

31

$\sigma = 4\%$ $\sigma = 1\%$

Typical
Perturbed
Ray

Unperturbed
Ray

Critical

X   X

- Contours of $n_e/n_c = x + \delta n\,(x, y, z)/n_c$ in intervals of 0.1
- Correlation length $h = 0.1$

TC1213

Fig. 18
Plane-parallel uniform-gradient plasmas with superimposed density fluctuations indicated by isodensity contours. Cases with rms fluctuation amplitudes of $\sigma/n_c = 0.01$ and 0.04 are shown. The correlation length h is chosen to be $h/L = 0.1$. Each frame shows how a typical ray wanders from the unperturbed path due to the given fluctuations.

the turning point, are reproduced. This focusing by the background density gradient gives the beam an elliptical profile.

A more quantitative comparison of the Monte-Carlo and statistical methods is shown in Fig. 21 where the rms angular radii (at the point of emerging from the plasma) are plotted as functions of the angle of incidence. The emerging beam profile is elliptical with principal axes in and normal to the unperturbed plane of refraction. Here, $\sigma/n_c = 0.01$ and $h/L = 0.1$. The scatter of the Monte-Carlo points is due to the limited number (27) of trials taken per run. The agreement of these
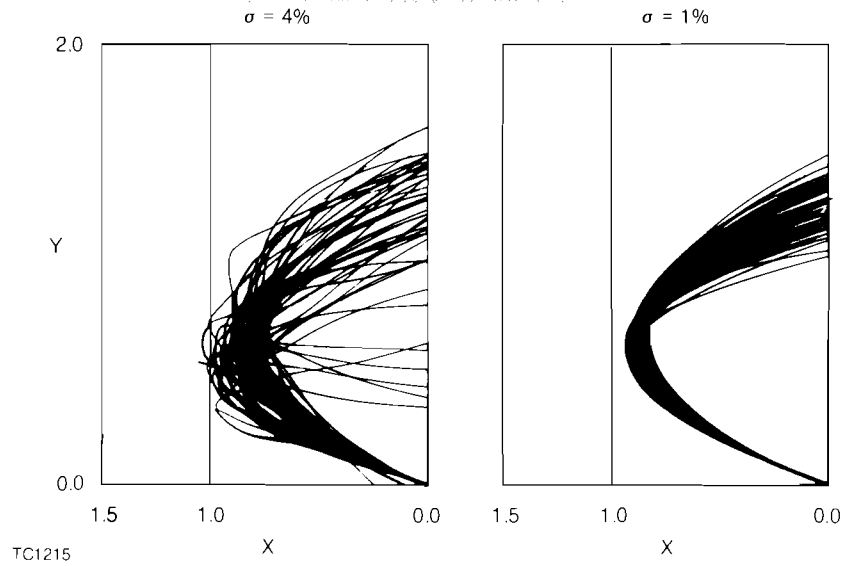
Fig. 19
Bundles of 49 rays propagating in the same conditions illustrated in Fig. 18. Each ray shown propagates according to a statistically independent sample of the fluctuation distribution. The bundles are Monte-Carlo representations of a spreading beam.
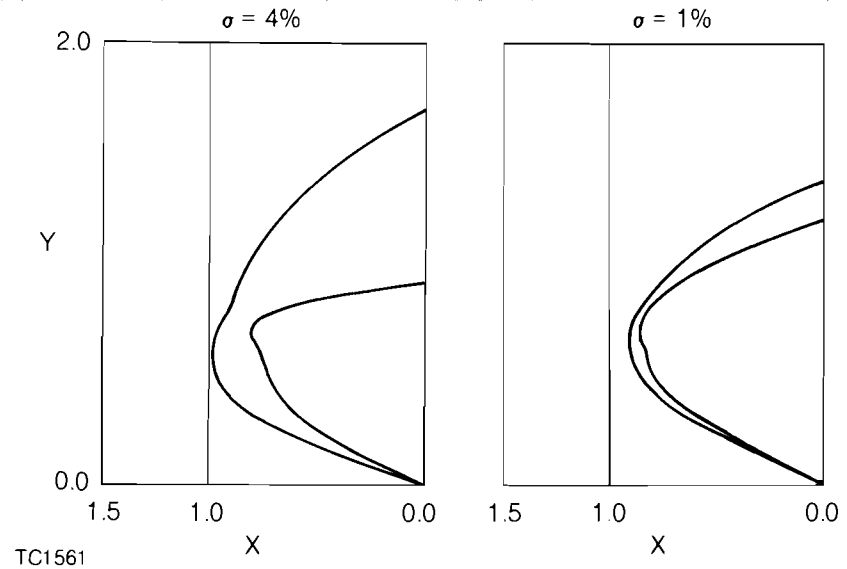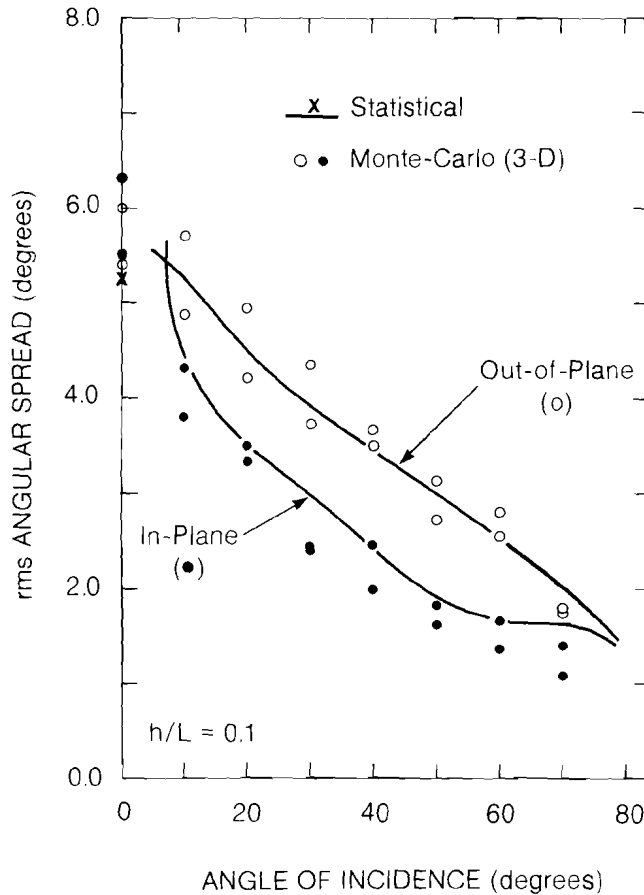

Fig. 20
The outlines of the rms ray-displacement envelopes obtained from the statistical ray-tracing theory for the same conditions as in Figs. 18 and 19. The agreement between the statistical and Monte-Carlo calculations is apparent from the superposition of the corresponding frames of this figure and Fig. 19.

33

Fig. 21
The principal rms angular radii of the elliptical profile of the beam (at the point where it emerges from the slab) is plotted as a function of the angle of incidence of the initial pencil beam. The conditions $\sigma/n_c = 0.01$ and $h/L = 0.1$ are assumed. The statistical ray-tracing results fall within the scatter of the dots representing Monte-Carlo calculations.

points with the statistical theory curves is well within this scatter. The spatial width of the emerging beam obtained by both methods is plotted in Fig. 22, where the agreement between the statistical curve and the scattered Monte-Carlo points is also apparent. The isolated "X" in both Figs. 21 and 22 represents a statistical result for the singular normal-incidence case. As the initial beam approaches normal incidence, the distance of closest approach to the critical surface of the unperturbed ray path becomes smaller, and the small-perturbation condition, Eq. (3a), is eventually violated. The calculation of the isolated normal-incidence point avoids this difficulty by simply neglecting any beam spreading that occurs within one correlation length of the unperturbed critical surface. This *ad hoc* "fix-up" affects only a small fraction of the total ray path, so it is not unreasonable that the result should be in rough agreement with the Monte-Carlo results.

According to the σ-scaling of the angular spreading rate given by Eq. (6), the angular and spatial widths given in Figs. 21 and 22 should scale linearly with σ. This scaling is verified in Fig. 23 for the spatial
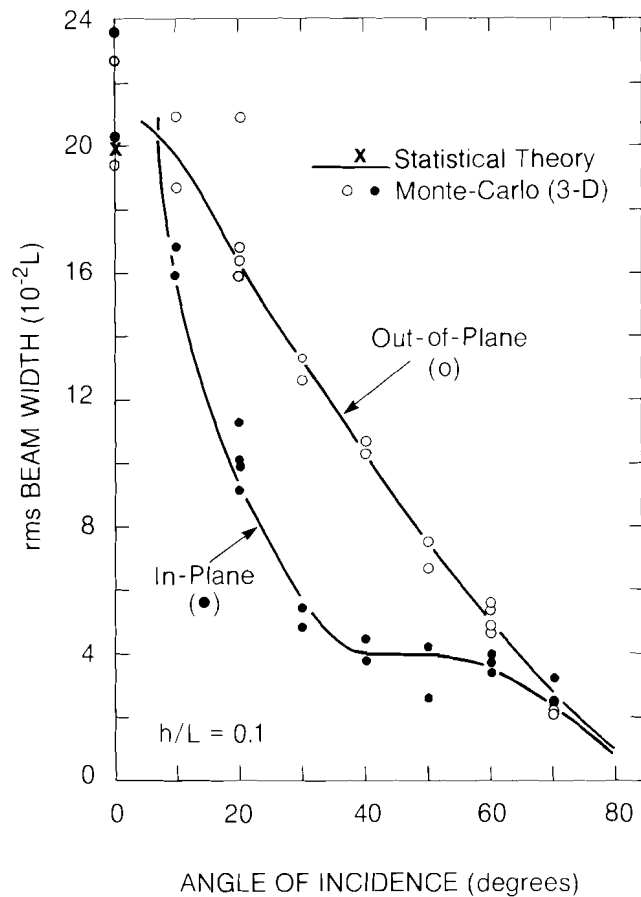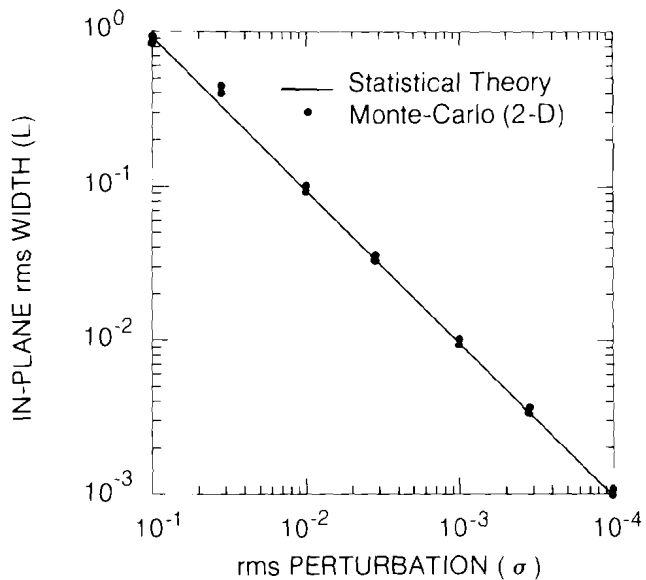
ANGLE OF INCIDENCE (degrees)

TC1220

Fig. 22
Same as Fig. 21, except that the principal rms spatial radii, rather than angular radii, are plotted.

beam width in the plane of refraction for an angle of incidence of 20°. The Monte-Carlo runs verify this linear scaling up to a fluctuation level of $\sigma/n_c \sim 0.1$. At the point along the unperturbed ray most closely approaching the critical surface, density fluctuations of this magnitude typically give index-of-refraction fluctuations comparable to the unperturbed index of refraction, which violates the small-perturbation condition, Eq. (3b). The verification of linear scaling for such large fluctuation amplitudes is a strong indication of the reliability of the statistical method.

It has been observed experimentally that angle-of-incidence dependences of energy absorption efficiencies are weaker than predicted by simple analytical models.[9] In some cases, such an effect may be attributable to density fluctuations. Figure 24 shows the absorption fraction for inverse bremsstrahlung for the plane-parallel, uniform-gradient plasma considered above, plotted as a function of the angle of incidence. The circles represent individual two-dimensional Monte-Carlo calculations for $\sigma/n_c = 0.05$ and $h/L = 0.1$. These are to

Fig. 23
The rms width, in the unperturbed plane of refraction, of the emerging beam plotted as a function of the rms density-fluctuation amplitude for an angle of incidence of 20° and for $h/L=0.1$. The predicted linear scaling of the beam width with the fluctuation amplitude is verified by Monte-Carlo calculations, up to a fluctuation level of $\sigma/n_c =0.1$.

TC1217

Fig. 24
Monte-Carlo (circles) and statistical ray-tracing (dashed curve) estimates of the inverse-bremsstrahlung absorption fraction are plotted (left-hand scale) as functions of the angle of incidence for the $\sigma/n_c = 0.05$, $h/L = 0.1$ case. The absorption coefficient is chosen to give 80% absorption at normal incidence for the $\sigma = 0$ result shown by the solid curve. The statistical estimate of the absorption is obtained using penetration-depth distribution results represented by the upper-boundary and lower-boundary curves (right-hand scale).
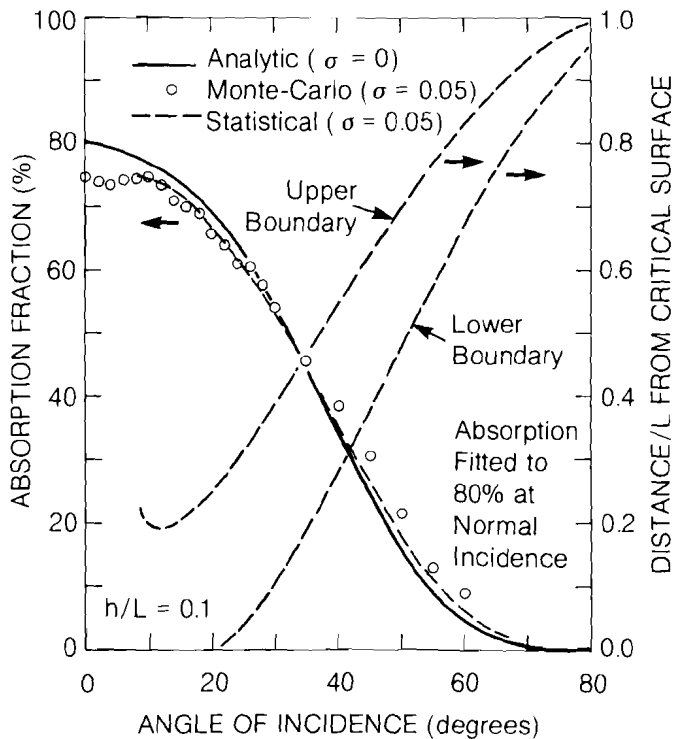
TC1218

be compared with the solid curve obtained analytically for the $\sigma = 0$ case.[12] In these calculations, the absorption coefficient was set such that 80% absorption would be obtained for normal incidence with $\sigma = 0$. The pair of dashed curves, read with the right-hand scale, gives the statistical theory results for the upper and lower rms beam boundaries at the point of closest approach to the critical surface, as a function of angle of incidence. The leveling of the Monte-Carlo angular dependence occurs at angles of incidence below about 15°, roughly where the statistical theory predicts a significant concentration of rays grazing the critical surface, a region accessible only to normally incident rays in an unperturbed plasma. Further decreases in the angle of incidence do not increase the concentration of near-critical rays significantly, just as if the beam were incident on the unperturbed plasma with an initial angular radius of about 15°.

The dashed absorption curve in Fig. 24 is a simple statistical-theory estimate of the change in the absorption efficiency due to the given fluctuations. Since the inverse-bremsstrahlung absorption cross section increases rapidly with electron density, it is assumed that the energy absorbed from a ray is most strongly dependent on the maximum penetration depth and less sensitive to the shape of the path, as long as the perturbed paths remain reasonably smooth. The statistical estimate is obtained by convolving the analytical zero-fluctuation result with a penetration depth distribution obtained from the statistical calculations. As can be seen in Fig. 24, this statistical estimate gives results similar to the Monte-Carlo results. The crudeness of the quantitative agreement is not unexpected, given the simplicity of the estimate. Nevertheless, both the statistical and Monte-Carlo calculations give curves that cross the zero-fluctuation result near a 35° angle of incidence, and the distinct flattening of the angle-of-incidence dependence of the statistical results occurs very near where Monte-Carlo results suggest. Closer agreement would certainly be obtained by making fuller use of the statistical ray distribution over the entire path of the spreading beam. This has yet to be done. It should be emphasized, however, that the statistical absorption-efficiency results are encouraging as examples of what can be obtained using relatively simple estimates, without resorting to lengthy Monte-Carlo calculations.

Summary

The most significant result of this work is the application of statistical ray-tracing techniques to strongly refracting plasmas. The agreement obtained between the statistical and Monte-Carlo methods verify the reliability of the statistical results. It should be noted that density fluctuations as small as a few percent of the critical density with about ten correlation lengths per scale length can result in angular spreads in reflected beams of the order of 10°. The statistical method offers a means to obtain estimates of density fluctuation effects that are otherwise obtainable only by time-consuming Monte-Carlo methods. Finally, although we have concentrated on laser-fusion applications, it should be stressed that theories of wave propagation in random media are of general applicability. The work we have presented is potentially applicable to a number of other areas.